Applied Ocean Research 39 (2012) 20–30

Contents lists available at SciVerse ScienceDirect

Applied Ocean Research

journal homepage: www.elsevier.com/locate/apor

Wave modeling performance in the Gulf of Mexico and Western Caribbean: Wind reanalyses assessment

Christian M. Appendini[a,*], Alec Torres-Freyermuth[a], Fernando Oropeza[b], Paulo Salles[a], Jose López[a], E. Tonatiuh Mendoza[a]

[a] *Laboratorio de Ingeniería y Procesos Costeros, Instituto de Ingeniería, Universidad Nacional Autónoma de México, Puerto de Abrigo s/n, 92718 Sisal, Mexico*
[b] *Centro de Ciencias de la Atmósfera, Universidad Nacional Autónoma de México, Cd. Universitaria, 04360 Mexico City, Mexico*

ARTICLE INFO

Article history:
Received 4 October 2011
Received in revised form 14 August 2012
Accepted 22 September 2012

Keywords:
Wave modeling
Wave hindcast
Wind reanalysis
Gulf of Mexico

ABSTRACT

This paper evaluates the wave modeling performance in the Gulf of Mexico and Western Caribbean Sea employing three different wind reanalysis data. Wind reanalysis is employed as the main forcing in wave generation/propagation numerical models. While the National Centers for Environmental Prediction (NCEP)/ National Center for Atmospheric Research (NCAR) and the European Centre for Medium-Range Weather Forecasts (ECMWFs) ERA-40 reanalyses have been previously assessed in the performance for wave modeling, ECMWF's ERA-interim and in particular NCEP's North American Regional Reanalysis (NARR) are more recent reanalyses. They both provide better resolution and description of the wind fields and have not been evaluated for long-term wave modeling. Therefore, the aim of this work is the assessment of the three different wind reanalyses on the wave hindcast performance. Attention is drawn on the wind reanalysis capability for predicting both mean and extreme wave conditions during two different periods: (i) an anomalous year where cyclonic events dominate the extreme wave climate in the region (2005); and (ii) a year with the wave climate dominated by synoptic events (2006). A third generation wave model, forced by the different wind reanalysis data, is calibrated with National Data Buoy Center (NDBC) buoys observations. Wind reanalysis data allow a consistent implementation of third generation wave models in order to predict the mean wave climate (correlation coefficient ~0.84 for NCEP/NCAR, 0.94 for ERA-interim, 0.92 for NARR) for applied ocean studies. Numerical results revealed that both ERA-interim and NARR improve the wave modeling performance with respect to NCEP/NCAR (for extreme and non-extreme conditions), whereas the high- (spatial and temporal) resolution NARR data are more suitable for modeling extreme cyclonic events (i.e., hurricanes) in this region.

1. Introduction

The direct impact of ocean waves on human activities (e.g., offshore oil and gas extraction, navigation, and beach recreation) provides endless examples for emphasizing the need to understand their generation and propagation processes. Indeed, the efforts to characterize wave conditions can be traced to ancient times, but it is only during the second half of the 20th century when a great leap forward was taken in the understanding of wave generation and propagation mechanisms. Together with the development of computers the progress and wide use of numerical models started, providing an excellent tool for wave hindcasting and forecasting. Furthermore, numerical models provide a tool to complement the low-spatial coverage of measured data. Moreover, the development of numerical models has led to advanced third generation (3G) wave models [1–4] which are used nowadays for wave characterization, allowing the generation of wave databases for ocean areas back to those years where no wave data existed, i.e., wave hindcast.

The main driving force for 3G wave models are the wind fields. Despite the existence of highly sophisticated wave models, the accuracy of wave hindcast will depend on the accuracy of the forcing data, i.e., wind fields, employed to drive the models [5]. Thus, in order to perform long-term wave hindcast studies, accurate wind field descriptions which cover the area of interest in both time and space are sought. Such datasets are now available through the atmospheric reanalysis in which numerical models using data assimilation techniques provide data sets with no inhomogeneities regarding the analysis techniques [6]. Moreover, the dependence of the wave model accuracy to the quality of the input wind field has led to assessments on the quality of the National Centers for Environmental Prediction (NCEP)/National Center for Atmospheric Research (NCAR) global reanalysis (hereafter referred as NCEP). These assessments were based on the use of the wind fields for driving a well validated 3G wave model, resulting in an exhaustive evaluation of the wave model results against all available wave measurements [7].

While several authors have focused on the long-term wave hindcast using wind reanalysis data and providing an assessment of the

* Corresponding author. Tel.: +52 9999266500x26722.
E-mail address: CAppendiniA@iingen.unam.mx (C.M. Appendini).

0141-1187/$ - see front matter
http://dx.doi.org/10.1016/j.apor.2012.09.004

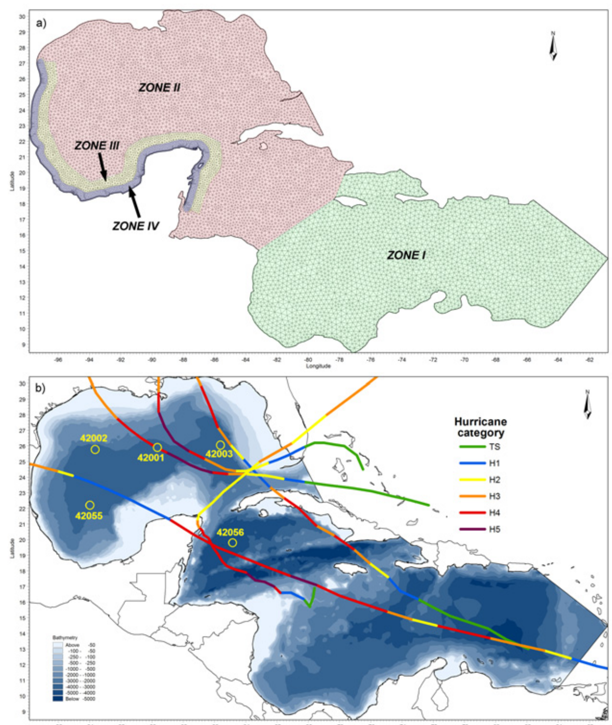

Fig. 1. (a) Computational model mesh showing the different resolution areas and (b) bathymetry from ETOPO-1 used for wave model simulations along with hurricane tracks and intensities (from NHC/Best-Track) for selected events and location of NDBC buoys used for evaluating the wave hindcast.

wind performance, downscaling wind data for wave modeling [8–11] or even intercomparing NCEP and the European Centre for Medium-Range Weather Forecasts (ECMWFs) ERA-40 [12], there is limited assessment available including the more recent ECMWF's ERA-interim dataset and/or NCEP's North American Regional Reanalysis (NARR). For instance, Caires et al. [13] provide a comprehensive analysis of different wind reanalyses, but even in their work, ERA-interim and NARR reanalyses were not considered. Moreover, while ERA and NCEP products have been extensively used in wave modeling, the NARR data have only a few wave hindcast applications dealing with short term simulations [14–16]. In view of the availability of NARR data, it was considered relevant to do the assessment as presented in this work. The recently released Climate Forecast System Reanalysis (CFSRR) [17] is a global reanalysis in a much finer resolution than other global reanalyses, but has a slightly coarser spatial resolution than the NARR. Therefore, considering the area of study (Fig. 1), the assessment of the NARR was considered more relevant for the Gulf of Mexico (GoM) and Western Caribbean Sea (WCS).

The study area (GoM and WCS) receives the effect of extreme wind waves generated by two different meteorological systems: (i) mid-latitude anticyclonic systems generating cold fronts known in vernacular language as *Nortes* due to its marked northerly approach to the Mexican GoM coast, and (ii) low pressure systems known as Tropical Cyclones (including tropical depressions, tropical storms and hurricanes), most of them approaching the area from the Caribbean Sea (CS). From hindcast studies presented in the literature it can be inferred that large scale meteorological systems such as *Nortes* are well represented by wind reanalyses, but it is not the case for mesoscale meteorological systems such as hurricanes.

In this work, an assessment of wave modeling performance using wind fields of the three different atmospheric reanalyses covering the study area is performed. Two years (2005 and 2006) of wind waves are simulated and compared against measurements from different National Data Buoy Center (NDBC) buoys. While an assessment is done over long-term hindcast, attention is also drawn to an assessment of extreme events, since the inaccuracy of low occurrence extreme events is shadowed by the accuracy of the highly occurring normal wave events in the long-term assessment. It is important to point out that the wind fields used in the study were used *"as is"*, i.e., as provided by the developers. Thus, the intention is to present an assessment which is not biased by further improvement of the data, leading to prohibitively expensive and time consuming methods [18] for long-term hindcast with applied purposes. As such, the assessment presented herein is useful for anyone who desires to use the data as available.

The outline of this paper is the following. A description of the methodology is given in Section 2. An assessment of the wave hindcast using the different reanalyses is given in Section 3. Finally, concluding remarks are drawn in Section 4.

2. Methodology

In order to evaluate the performance of different wind reanalyses for wave hindcasting in the GoM and WCS, a third generation model has been implemented in the study area. This area was selected for the following reasons: (i) the area is covered by the three most widely used wind reanalyses, (ii) the area experiences both high vorticity extreme wind events (hurricanes) and low vorticity extreme winds (*Nortes*), (iii) the area is not significantly influenced by "long distance" swells and all wind waves are generated inside the basins, and (iv) it provides valuable wave information for Mexican waters, covered by monitoring programs sparse in time and space. The procedure followed to evaluate the performance of different reanalyses is described below.

2.1. Wave model description

The wave model used for the assessment of the wind reanalysis was the third generation spectral wave model MIKE 21 SW [1]. This model is based on unstructured meshes and simulates the growth, decay, and transformation of wind generated waves and swells in coastal and offshore regions. The MIKE 21 SW model is formulated in terms of mean wave direction, θ, and the relative angular frequency, σ, where the action density, $N(\sigma,\theta)$, is related to the energy density, $E(\sigma,\theta)$ by:

$$N(\sigma,\theta) = \frac{E(\sigma,\theta)}{\sigma}$$

For large applications, such as the one presented in this study, the wave action balance equation is formulated in spherical coordinates, where the evolution of the wave spectrum in the position given by latitude $\varnothing$ and longitude λ at a particular time t and is given as follows:

$$\frac{\delta N}{\delta t} + \frac{\delta}{\delta \varnothing} c_{\varnothing} N + \frac{\delta}{\delta \lambda} c_{\lambda} N + \frac{\delta}{\delta \sigma} c_{\sigma} N + \frac{\delta}{\delta \theta} c_{\theta} N = \frac{S}{\sigma}$$

The energy source term S represents a superposition of energy source/sink functions that describe the multiple physical phenomena during wave generation and transformation. For details regarding source terms, discretization of the governing equation, time integration, and model parameters readers are referred to Sørensen et al. [1].

While whitecapping is the least understood part on wave evolution, it has been, and still is, the tuning knob of any wave model [19] and hence deserves further attention. MIKE 21 SW uses the WAM-Cycle 4 formulation [4], based on the theory of Hasselmann [20], where whitecapping dissipation is assumed to be a result of pressure induced decay reformulated in terms of wave number [21] (i.e.,

Table 1
Computational grid definition.

Zone	Maximum area (degrees^2)	Maximum approximate size of element side (km)
I	0.06	40
II	0.03	28
III	0.014	19
IV	0.005	12

Table 2
Wind data grid definition for the three different reanalysis.

Reanalysis	Left-down corner	Dx	Dy	Dt
NCEP	−99.3750, 6.6666	1.875°	1.9047°	21,600 s (6 h)
ERA[a]	−99, 6	1.5°	1.5°	21,600 s (6 h)
NARR	−98.5, 7.1250	0.375°	0.375°	10,800 s (3 h)

[a] Spatial resolution is publicly available at 0.75° since December 2011.

WAM-Cycle 3), and an adjustment of the dissipation source function based on the wind input description by Janssen [22]. According to Ardhuin et al. [23] WAM-Cycle 4 formulation is adjusted to close the wave energy balance, but lacks of physical justification. However, this formulation is widely used in most numerical wave models, such as SWAN [24] and WAVEWATCH III [3] owing to the simplicity of its implementation. While more recent parameterizations have a more physical justification of the whitecapping process (e.g., van der Westhuysen et al. [25] and Ardhuin et al. [23]), the WAM-Cycle 4 formulation is still the default in 3G wave models. As such, a recent work by Siadatmousavi et al. [16] evaluates Cycle 3 and Cycle 4 formulations for the GoM, giving evidence of their current use. One of the flaws in the WAM-Cycle 4 formulation is that it applies the whitecapping to the whole spectrum, producing an over-prediction in swell dissipation [19]. However, the present study considered that seas are dominant due to the basin limits blocking distant swells and hence the formulation is an appropriate approximation. Considering the above, whitecapping was used as the main calibration parameter in this work.

It is relevant to mention that MIKE 21 SW does not account for a growth saturation limit in relation to wind speed, so that overestimation of wave height can result for young seas under high wind speeds, i.e., hurricanes [26].

2.2. Computational mesh

The computational mesh covers the full extent of the GoM and the CS, dividing the domain in to four main areas with different element sizes (Fig. 1a). For the GoM and the northwestern CS a maximum element area of 0.03° was used (zone II), while for the southeastern CS a maximum element area of 0.06° was selected (zone I). The higher mesh resolution was selected for the coastal area of Mexico (maximum element area of 0.005°; zone IV), due to the interest of the researchers in this particular region. Table 1 shows the corresponding element size (in km) for each of the maximum area (in degrees) defined in the model domain. The bathymetry data employed correspond to the NOAA's ETOPO1 [27], which are considered as the most suitable data source for the whole computational domain. The final bathymetry for the domain and the developed mesh covers 8.25°–30.5°N latitude and 98°–60.75°W longitude. The Atlantic Ocean (Fig. 1b) is not included in the computation domain, so that the model is limited to the east by the Antilles Islands and the Bahamas as shown in Fig. 1. Please note that there are no open boundaries between islands, assuming that there is no influence of Atlantic swell into the study area which was found to be a reasonable assumption.

The Mexican coastline was defined with a 3.5 km resolution which gradually increases to a maximum element size of 12 km at a distance of 60 km from the shore. The US coastline has an approximate resolution of 20 km and the rest of the coastline has a resolution of 25 km (as obtained from NGDT/NOAA's coastline extractor).

2.3. Model setup

The wave model was setup with the fully spectral and instationary time formulations. A logarithmic spectral discretization was used with a minimum frequency of 0.055 Hz, 25 frequencies, and a frequency increment factor of 1.1 (this was based on wave period buoy measurements in the area for the period from 1979 through 2008). The directional discretization is done for 360° divided in to 16 directions (based on model performance vs. computational time, following suggestion of recommended values for seas [28]). The time step, based on a multi-sequence integration step, is specified with a minimum value of 0.01 s and maximum value of 10,800 s, whereas the actual time step used in each calculation is based on the CFL condition.

2.4. Wind forcing and simulated cases

The wind reanalyses tested in this work are the NCEP [29], ERA-interim [6,30], and NARR [31] reanalyses. Table 2 shows the spatial- and temporal-resolution for each reanalysis. It should be noted that the ERA-interim data at 0.75° spatial resolution were made publicly available during December 2011 and hence this study was carried out with the available public data resolution before that date (i.e., 1.5°). The 10 m wind components from the three different reanalyses were employed as the forcing for the numerical model.

The simulation periods were selected in order to evaluate the model performance during both normal and extreme conditions. While the former are well represented in wind reanalyses, such is not the case with the latter (i.e., extreme wind conditions) for cyclonic events characterized by high vorticity of intense and rapidly changing wind fields. A description of extreme events affecting the study area is given below.

Nortes usually occur September through April and are part of synoptic scale disturbances from mid-latitudes characterized by a cold front passage, generating sustained winds of about 30 m s^{-1} and associated with high pressure systems frequently originated at the Rocky Mountains in the USA [32]. The duration of the effects of a *Norte*, varies from one day to two weeks [33], having an important impact on the oil industry, fisheries, maritime transport, tourism and other activities in the GoM. On the other hand, hurricanes are the most extreme climate events that occur in the study area. The North Atlantic Tropical Cyclones season runs from June 1st to November 30th, with a yearly average of 11.1 named events. The peak of the season is from mid-August to late October, while September is the month with the highest number of Tropical Cyclones directly affecting the Mexican coasts [34]. In order to allow the assessment of both mean and extreme wave conditions under two different scenarios regarding the nature of extreme conditions, years 2005 and 2006 were selected. In the following there is a description of those years in relation to the extreme events.

Year 2005 was selected as a first simulation period due to the very active hurricane season, which in terms of accumulated cyclone energy had a record value of 256% above the long-term mean (a comprehensive description of this hurricane season is presented in Beven et al. [35] and Trenberth and Shea [36]). This year has the record in terms of the number of named storms (27 tropical and one subtropical storm), 15 of them became hurricane of which 7 became major hurricane (category 3 or higher on the Saffir–Simpson hurricane scale). Moreover, four hurricanes (Emily, Katrina – most damaging storm in history, Rita – most intense storm in the GoM, Wilma – most intense Atlantic storm ever registered) reached category 5 (maximum

Table 3
Statistical parameters for 10 m wind speed comparing different wind reanalysis data and in situ observations from NDBC buoys.

Buoy Id	Stat. param.	2005				2006				2005–2006			
		NDBC	NCEP	ERA	NARR	NDBC	NCEP	ERA	NARR	NDBC	NCEP	ERA	NARR
42001	No. obs.			2919[a]				2919[a]				2838[a]	
	Mean	6.10	5.83	5.65	5.94	6.13	5.80	5.58	5.79	6.12	5.73	5.55	5.86
	Median	5.80	5.65	5.46	5.82	5.90	5.55	5.35	5.54	5.80	5.52	5.36	5.66
	STD	3.38	2.87	2.76	2.98	3.20	2.97	2.81	3.02	3.29	2.91	2.76	3.00
	Corr. coef.	N/A	0.71	0.86	0.82	N/A	0.78	0.93	0.87	N/A	0.76	0.89	0.84
42002	No. obs.			2919[a]				[b]				2919[a]	
	Mean	6.18	6.23	5.72	5.95	[b]	6.26	5.82	6.09	6.18	6.16	5.70	6.02
	Median	6.00	5.96	5.56	5.86	[b]	5.90	5.53	5.83	6.00	5.80	5.51	5.85
	STD	2.95	2.89	2.64	2.76	[b]	3.00	2.75	2.92	2.95	2.91	2.66	2.84
	Corr. coef.	N/A	0.70	0.89	0.82	N/A	N/A	N/A	N/A	N/A	0.70	0.89	0.82
42003	No. obs.			2601[a]				2919[a]				5520[a]	
	Mean	6.17	5.85	5.68	5.71	5.67	5.54	5.25	5.20	5.91	5.63	5.40	5.46
	Median	6.00	5.66	5.54	5.46	5.10	5.02	4.75	4.71	5.60	5.24	5.08	5.06
	STD	3.11	3.04	2.88	3.16	3.14	2.88	2.73	2.77	3.13	2.94	2.79	2.98
	Corr. coef.	N/A	0.76	0.89	0.83	N/A	0.79	0.92	0.84	N/A	0.79	0.90	0.84
45055	No. obs.			1879[a]				2795[a]				4674[a]	
	Mean	6.23	6.17	5.76	5.46	6.47	6.08	5.85	5.47	6.37	6.03	5.75	5.46
	Median	6.10	6.04	5.66	5.34	6.20	5.75	5.60	5.33	6.20	5.79	5.57	5.33
	STD	2.56	2.50	2.11	2.21	2.79	2.84	2.38	2.50	2.70	2.61	2.20	2.36
	Corr. coef.	N/A	0.57	0.90	0.76	N/A	0.65	0.92	0.81	N/A	0.65	0.89	0.79
42056	No. obs.			1936[a]				1934[a]				3870[a]	
	Mean	6.79	6.30	6.43	5.77	6.16	6.05	6.12	5.40	6.48	6.14	6.25	5.59
	Median	6.40	6.34	6.27	5.60	6.10	5.96	6.11	5.32	6.30	6.08	6.13	5.46
	STD	3.33	2.26	2.38	2.75	2.40	2.10	2.02	2.27	2.92	2.16	2.19	2.53
	Corr. coef.	N/A	0.74	0.92	0.84	N/A	0.71	0.90	0.76	N/A	0.73	0.90	0.81

[a] Values correspond to observations at NDBC buoy.
[b] There are no observations for NDBC buoy 42002 during 2006.

1-min winds greater than 69.5 m s^{-1}), being the first time this had been observed in one season [35]. Eleven hurricanes had a direct impact over the GoM and/or the Mexican CS. It is well-known that NCEP wind reanalysis does not have a good representation of cyclone events. Therefore, that year was selected in order to investigate the effect of employing higher-resolution wind fields (i.e., NARR) on the wave model performance. With respect to large-scale meteorological systems, there were 14 *Nortes* in 2005 during the winter time, based on the definition of López-Méndez [37], 9 of them were between the months of January and April, and the other 5 were between November and December.[1]

On the other hand, year 2006 is characterized by a near average overall cyclone activity with accumulated cyclone energy of 90% the long-term mean (a detailed descriptions of the 2006 hurricane season can be found at Franklin and Brown [38]). For the matter of this study, the cyclone activity was low since in the GoM and the CS only Tropical Storm Alberto (period 10–14 June) crossed the GoM after its genesis in the northwest CS, and tropical storms Chris and Ernesto passed close to our model boundary, without having much effect over the GoM. Regarding large-scale meteorological systems, the 2006 winter season had a presence of 21 *Nortes*, based on the definition of López-Méndez [37], 12 of them between January and April, and the other 9 were between October and December. In this study, that year is considered representative of larger scale meteorological events, which should be well represented in the wind reanalysis, so that the statistic measures can be analyzed without the influence of major cyclonic events.

A comparison between wind reanalyses and NDBC data is carried out considering the buoy measurements as provided by NDBC without reducing observational error and/or further quality control (information regarding the measuring technique and the quality control of the data is found at NDBC [39]). Table 3 shows statistical parameters at selected NDBC locations (shown in Fig. 1b) for the different reanalysis wind speed data and in situ measurements. The comparisons are made 6 hourly for NCEP/ERA and 3 hourly for NARR, consistent with data time step. Measured wind speed is better correlated to ERA ($r^2 \sim 0.89$), than to NARR ($r^2 \sim 0.82$), whereas the lowest correlations is for NCEP ($r^2 \sim 0.73$). For locations at NDBC buoys 42001 (northern GoM), 42055 (Campeche Sound) and 42056 (Mexican CS), representative of the study area, Fig. 2 shows the temporal *XY* scatter plots (shown as density) and quantile–quantile (QQ) scatter plots for wind speed for 2005 and 2006. As observed in the figures, wind speed is underestimated for tropical storm and higher wind speeds, only occurring during 2005 at buoys 42001 and 42056. While NCEP provides a very good estimate of wind speeds at buoy 42055 during 2005 and 2006, ERA and NARR show a slight underestimation at this location. During 2006, NCEP and NARR show an accurate estimation of wind speed at buoy 42001 while ERA slightly underestimates it. At buoy 42056 all three reanalyses slightly underestimates wind speeds during 2006. While there is some underestimation for wind speeds below tropical storm force (<17.5 m/s), it is clear that the highest disagreement

[1] López-Méndez defines a *Norte* as an atmospheric event characterized by reduced mean sea level pressure higher than 1020 hPa at coordinates 30°N, 100°W (over the continental USA, capturing the effect of the high pressure systems moving toward the GoM), with simultaneous winds speeds higher than 12 m s^{-1} at 20°N, 93.75°W (southern GoM, commonly affected by strong winds associated to high pressure systems) between September and April.

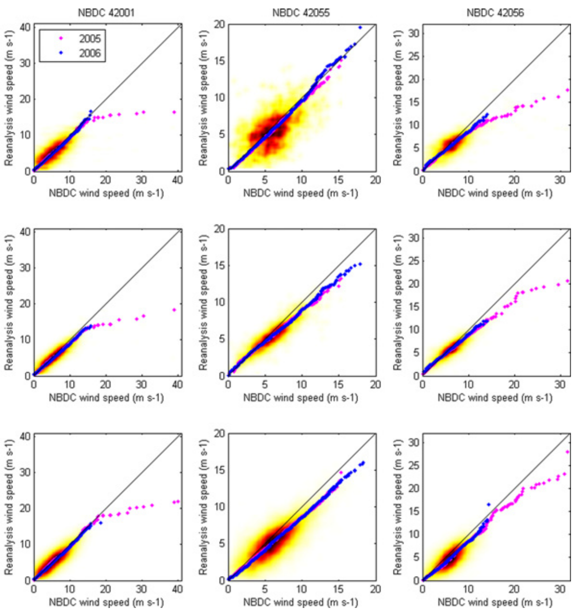

Fig. 2. Temporal (density contours) and QQ (dots) scatter plots of observed vs. simulated 10 m wind speed at different NDBC buoy locations during 2005 and 2006.

between reanalyses and observations occurs during tropical storms and hurricanes. On the other hand, all three reanalyses accurately resolves large-scale meteorological systems such as *Nortes*. It is worth to mention that while data assimilation is part of the wind reanalysis process, the underestimation of wind speeds during hurricanes is present at all locations. Wind direction is very well represented in all reanalyses (not shown).

2.5. Assessment of numerical results

The wave model was implemented for the two simulation periods using the three different wind reanalysis (NCEP, ERA and NARR). For each of the simulation an independent quality index analysis was performed to obtain the statistic values for bias, bias index (BI), RMS error, scatter index (SI) and correlation coefficient (r^2), as in Moeini and Etemad-Shahidi [40].

Statistical parameters can be employed for the model calibration, provide an overview of the accuracy of the results, and allows to evaluate the wave modeling performance for different reanalysis sets. Unfortunately, these parameters do not reflect the model performance during storm events, which represent a small sample in the whole universe of events, and whose errors are smoothed out over the entire year of the analysis. Thus, in order to assess the accuracy of the simulations during extreme events for both periods, independent analyses were performed over selected extreme events (i.e., Hurricanes and *Nortes*) listed in Table 4. Moreover, for the complete simulation periods such as visual inspection of time series during extreme events, quantile–quantile (QQ plots), and scatter (*XY*) plots are also shown.

The wave hindcast is compared against NDBC data from NOAA, which has a broad range of devices measuring wave conditions around the GoM and the CS. The buoys selected within the study area are located in deepwater in the upper GoM (42001, 42002, and 42003), the Campeche basin (42055), and the Yucatan Channel (42056) (see Fig. 1b). It is considered that buoys 42001, 42055, and 42056 characterize the different study area regions (Mid Gulf, lower Gulf and WCS, respectively), whereas buoys 42002 and 42003 allow the assessment of selected extreme events.

Table 4
Selected extreme events.

Event	Simulation period	Start	End
Dennis	2005	07/04	07/18
Emily	2005	07/11	07/21
Katrina	2005	08/23	08/31
Rita	2005	09/18	09/26
Wilma	2005	10/15	10/26
Norte 01	2006	02/11	02/15
Norte 02	2006	03/23	03/26
Norte 03	2006	11/15	11/18
Norte 04	2006	12/01	12/07

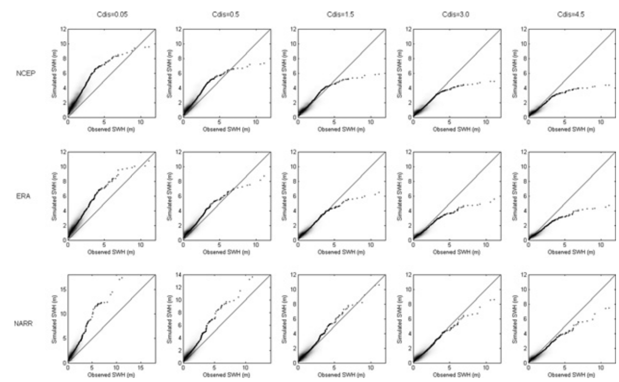

Fig. 3. Temporal (density contours) and QQ (dots) scatter plots of observed vs. simulated SWH at buoy 42001 during 2005 using varying C_{dis} coefficient.

2.6. Model calibration

While whitecapping is the main calibration parameter in wave models, it is acknowledged by the authors that scientific efforts should be oriented in developing whitecapping formulations to be representative of physical processes, which is not the aim of the present work. The model was driven by the different wind fields and the whitecapping coefficients, C_{dis} and $\mathrm{Delta}_{\mathrm{dis}}$, were used for the model calibration. The C_{dis} coefficient controls the overall dissipation rate, having a primary effect on wave height, while the $\mathrm{Delta}_{\mathrm{dis}}$ coefficient controls the weight of dissipation in the energy-action spectrum, so that its effect is shown over the wave period. Chao et al. [41] consider that tuning the wave model with wind fields from general atmospheric circulation models is not always optimal for more accurate hurricane winds. Therefore, based on this observation, a fine tuning with hurricane events was performed after a general tuning of the model.

The general tuning consists on using C_{dis} values between 0.005 and 4.5 (values between 1 and 4.5 fall within commonly used values and 0.005 was tested for sensitivity) in order to find the best fit with the data. Several tests were performed varying the $\mathrm{Delta}_{\mathrm{dis}}$ coefficient, finding a $\mathrm{Delta}_{\mathrm{dis}}$ value equal to 0.8 as the optimal for this region. The resulting significant wave height (SWH) scatter and QQ plots are shown in Fig. 3 for NDBC 42001 during year 2005. The results show that for values $C_{\mathrm{dis}} < 1$ the resulting SWH is overestimated even for small waves, which provides evidence of the lack of physical representation of the whitecapping processes (i.e., wind speeds producing such waves generate few whitecaps along the sea surface). For values greater than 3 the resulting SWH for ERA and NARR reanalyses, even for small SWH, is underestimated.

Subsequently, the fine tuning was performed running the model for both simulation periods using a $C_{\mathrm{dis}} = 1$, 1.5 and 2, where an optimal value of $C_{\mathrm{dis}} = 1.5$ and $\mathrm{Delta}_{\mathrm{dis}} = 0.8$ was determined from the simulations, which are close to the values established by Jose et al. [42] and Siadatmousavi et al. [15,16] for the GoM. This value proved

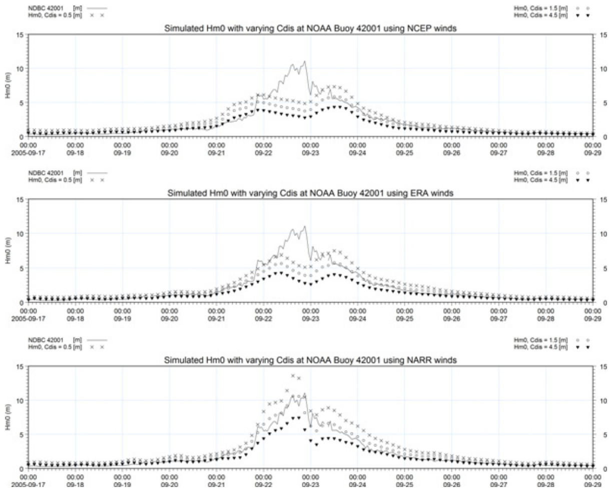

Fig. 4. SWH during Rita using varying C_{dis} coefficient for different wind reanalysis as forcing agent: NCEP (top), ERA (middle) and NARR (bottom).

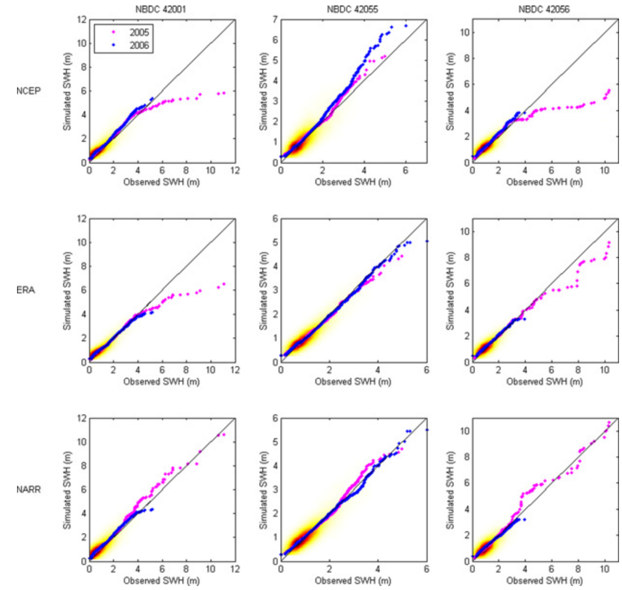

Fig. 5. Temporal (density contours) and QQ (dots) scatter plots of observed vs. simulated SWH at different NDBC buoy locations during 2005 and 2006.

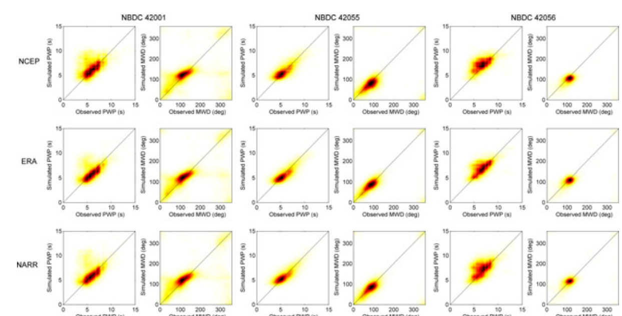

Fig. 6. Temporal (density contours) scatter plots of observed vs. simulated PWP and MWD values at different NDBC buoy locations during 2005–2006.

to be optimal for the three wind reanalyses, so that they were applied for all simulations. From Fig. 3 it may appear that the NCEP optimum value is around 3, but a detailed statistical analysis during 2006 (without a strong influence of hurricanes) shows an insignificant improvement with respect to $C_{dis} = 1.5$. Resulting SWH at buoy 42001 during hurricane Rita for different C_{dis} values is shown in Fig. 4, indicating that whitecapping (C_{dis} coefficient) can only be used as a calibration factor for a small compensation in the wind underestimation by the reanalysis.

3. Model-data comparisons

Time series at the NDBC buoys locations were extracted from model results and compared against observations. This section evaluates the model's performance for the different wind reanalyses.

3.1. Model-data comparison: simulated periods (2005 and 2006)

As a first estimate of the model performance, statistical parameters are computed to assess the accuracy compared with SWH observations at buoys 42001, 42002, 42003, 42055 and 42056 during 2005 and 2006 (Table 5). Model and measured data are highly correlated ($r^2 \sim 0.84$ for NCEP, $r^2 \sim 0.94$ for ERA, $r^2 \sim 0.92$ for NARR). This is expected since model calibration was focused on the energy content only. For a more thorough analysis of the accuracy of the simulations, temporal (shown as density) and quantile–quantile (QQ) scatter plots for buoys within the simulated area are shown for the northern GoM (42001), the Campeche Sound (42055), and the Mexican CS (42056) in Fig. 5. The wave data output of the model is every 3 h, so that comparisons were made with such time step. For the year 2005, characterized as a highly active hurricane year, there is a strong hurricane influence at buoys 42001 and 42056, and in a lesser extent at buoy 42055, which is consistent with the fact that most storm tracks (Fig. 1b) are far from this buoy location. Indeed, all wind reanalysis data provide highly correlated ($r^2 = 0.86$ for NECP, $r^2 = 0.94$ for ERA and $r^2 = 0.91$ for NARR) SWH estimates in the Campeche Sound during this year. On the other hand, there is an underestimation of approximately 40% for the highest SWH at 42001 for NCEP- and ERA-derived hindcast. This is also observed at 42056 when using NCEP and in a minor degree when using ERA. The use of NARR provides accurate results at the three locations reducing the difference between simulated and measured highest SWH to approximately 10%, despite the fact that a slight overestimation occurs at intermediate wave height cases.

For the year 2006 all reanalysis present a good agreement with observations, with slight overestimation of the mean wave climate at buoys 42001 and 42056. Most frequent events are well represented at buoy 42055 for the three reanalyses. Model performance can be improved for the most frequent waves by increasing the C_{dis} value. However, the latter will have an effect on the prediction of extreme SWH, particularly during 2005 hurricane's season.

It is concluded that the ERA and NARR reanalysis provides better SWH estimates than NCEP, which is corroborated with the statistical parameters presented in Table 5. Please note that the statistical parameters smooth out inconsistencies during the low occurrence extreme events, in that sense, the use of ERA data appears more accurate with respect to NARR. On the other hand, the QQ plots show that the NARR data provide more accurate results than ERA during extreme events. Therefore, considering both extreme and normal events, we can concluded that NARR data provide an overall better wave modeling results, providing accurate results for both mean and extreme events. Moreover, an assessment on the accuracy of peak wave period (PWP) and mean wave direction (MWD) of each of the simulations showed a good agreement with the data using the three different reanalysis (Fig. 6).

3.2. Model-data comparison: hurricane events

Fig. 7 shows the SWH, PWP, and MWD at buoy 42001 during hurricane Rita, where it is evident that NARR is the reanalysis that most accurately represent the observed values during such event,

Table 5
Statistical parameters for SWH comparing results using different wind reanalysis and in situ observations from NDBC buoys.

Buoy Id	Stat. param.	2005			2006			2005–2006		
		NCEP	ERA	NARR	NCEP	ERA	NARR	NCEP	ERA	NARR
	No. obs.		2891[a]			2906[a]			5797[a]	
	Mean obs.		1.16[a]			1.07[a]			1.11[a]	
	Mean sim.	1.37	1.25	1.37	1.37	1.22	1.33	1.37	1.24	1.35
42001	Bias	0.21	0.10	0.22	0.30	0.15	0.26	0.25	0.12	0.24
	Bias index	0.18	0.08	0.19	0.28	0.14	0.24	0.23	0.11	0.21
	RMS	0.55	0.40	0.42	0.50	0.29	0.38	0.52	0.35	0.40
	Scatter Index	0.48	0.34	0.37	0.46	0.27	0.36	0.47	0.31	0.36
	Corr. coef.	0.83	0.91	0.92	0.88	0.95	0.93	0.85	0.93	0.93
	No. obs.		2480[a]			[b]			[b]	
	Mean obs.		1.24[a]							
	Mean sim.	1.41	1.23	1.36						
42002	Bias	0.16	−0.01	0.11						
	Bias index	0.13	−0.01	0.09						
	RMS	0.48	0.28	0.39						
	Scatter index	0.38	0.22	0.32						
	Corr. coef.	0.82	0.92	0.88						
	No. obs.		2593[a]			2909[a]			5502[a]	
	Mean obs.		1.18[a]			1.07[a]			1.12[a]	
	Mean sim.	1.15	1.08	1.13	1.07	0.98	1.02	1.11	1.03	1.07
42003	Bias	−0.03	−0.10	−0.05	0.00	−0.09	−0.06	−0.02	−0.10	−0.05
	Bias index	−0.03	−0.09	−0.04	0.00	−0.09	−0.05	−0.01	−0.09	−0.05
	RMS	0.49	0.36	0.36	0.39	0.29	0.32	0.44	0.32	0.34
	Scatter index	0.41	0.30	0.30	0.36	0.27	0.30	0.39	0.29	0.30
	Corr. coef.	0.81	0.91	0.91	0.87	0.94	0.92	0.85	0.92	0.91
	No. obs.		1854[a]			2727[a]			4581[a]	
	Mean obs.		1.15[a]			1.18[a]			1.16[a]	
	Mean sim.	1.23	1.15	1.20	1.29	1.18	1.21	1.27	1.17	1.21
42055	Bias	0.09	0.01	0.05	0.11	0.01	0.04	0.10	0.01	0.04
	Bias index	0.08	0.01	0.04	0.10	0.00	0.03	0.09	0.01	0.04
	RMS	0.38	0.24	0.29	0.47	0.25	0.28	0.44	0.25	0.28
	Scatter index	0.33	0.21	0.25	0.40	0.21	0.23	0.38	0.21	0.24
	Corr. coef.	0.86	0.94	0.91	0.83	0.94	0.92	0.84	0.94	0.92
	No. obs.		1878[a]			1889[a]			3767[a]	
	Mean obs.		1.27[a]			1.12[a]			1.20[a]	
	Mean sim.	1.42	1.39	1.33	1.38	1.29	1.21	1.40	1.34	1.27
42056	Bias	0.15	0.12	0.06	0.26	0.17	0.09	0.20	0.14	0.08
	Bias index	0.12	0.10	0.05	0.23	0.15	0.08	0.17	0.12	0.07
	RMS	0.65	0.34	0.37	0.36	0.25	0.28	0.53	0.30	0.33
	Scatter index	0.51	0.27	0.29	0.32	0.22	0.25	0.44	0.25	0.27
	Corr. coef.	0.78	0.95	0.94	0.89	0.94	0.87	0.80	0.95	0.92

[a] Values correspond to observations at NDBC buoy.
[b] There are no observations for NDBC buoy 42002 during 2006.

whereas a significant underestimation of SWH is presented for the NCEP and ERA reanalysis. The statistical parameters (i.e., bias index, scatter index, and correlation coefficient) for the selected hurricane events at different buoy locations are shown in Table 6. The bias index indicates that for most events there is a slight overestimation on SWH and in general ERA provides better estimates. The scatter index is generally better for the NARR and ERA reanalyses, as well as the correlation coefficient, which is significantly lower for the NCEP reanalyses in most events and locations.

Furthermore, in order to provide a visual representation of time-dependence of the different wave parameters (i.e., PWP, SWH and MWD) during the event, Fig. 8 shows the time series for the selected events at a selected location, where the y axis represent the SWH (value given at vector origin), PWP is represented by vector length and MWD by vector azimuth. As shown in the figure, NARR provides the best representation of the waves generated by the selected hurricane events, except during Rita at buoy 42002 (Fig. 8e) and hurricane Emily at 42056 (Fig. 8g). On the other hand, the NARR reanalysis provides extremely accurate wave parameters during Rita at buoy 42001 (Fig. 8b), Dennis at buoy 42003 (Fig. 8c), Katrina at buoy 42003 (Fig. 8d) and Wilma at buoy 42056 (Fig. 8h). During Katrina at buoy 42001 (Fig. 8a) there is a slight overestimation of SWH and during Emily at buoy 42055 (Fig. 8f) the MWD and PWP are not as accurate.

Table 6
Statistical parameters for SWH comparing results using different wind reanalysis and in situ observations from NDBC buoys during selected events.

Event	Buoy	No. obs.	Bias index			Scatter index			Correlation coefficient		
			NCEP	ERA	NARR	NCEP	ERA	NARR	NCEP	ERA	NARR
	42001	18	−0.15	−0.04	0.22	0.25	0.14	0.25	0.66	0.84	0.89
Dennis	42003	27	−0.02	0.06	0.13	0.52	0.35	0.27	0.53	0.78	0.91
	42055	30	0.23	0.02	0.13	0.30	0.18	0.22	0.86	0.92	0.89
	42001	34	0.13	0.10	0.24	0.37	0.24	0.34	0.72	0.90	0.94
Emily	42003	23	−0.23	−0.22	−0.03	0.43	0.34	0.12	0.44	0.83	0.94
	42055	19	0.09	−0.09	−0.13	0.23	0.25	0.23	0.67	0.76	0.84
	42056	48	0.07	0.00	−0.08	0.18	0.14	0.20	0.71	0.79	0.87
	42001	30	−0.19	−0.04	0.15	0.49	0.16	0.21	0.67	0.96	0.97
Katrina	42002	21	0.22	0.25	0.37	0.43	0.42	0.51	0.35	0.59	0.60
	42003	16	−0.72	−0.24	0.02	1.19	0.47	0.12	0.67	0.93	0.99
Rita	42001	40	−0.21	−0.24	0.06	0.64	0.58	0.19	0.68	0.82	0.96
	42002	36	0.22	0.17	0.31	0.41	0.23	0.41	0.65	0.96	0.96
	42001	50	0.18	0.15	0.26	0.26	0.23	0.31	0.90	0.89	0.88
	42002	39	0.22	0.13	0.27	0.35	0.19	0.32	0.66	0.88	0.84
Wilma	42003	57	−0.08	−0.15	0.06	0.30	0.31	0.32	0.86	0.85	0.84
	42001	23	0.03	0.03	−0.01	0.29	0.07	0.11	0.75	0.99	0.96
Norte 01	42003	24	0.03	0.08	−0.01	0.18	0.12	0.10	0.87	0.97	0.95
	42055	23	0.14	−0.03	-0.03	0.37	0.21	0.23	0.78	0.94	0.93
	42001	19	0.23	0.04	0.17	0.39	0.16	0.24	0.57	0.89	0.86
Norte 02	42003	23	0.23	0.02	0.06	0.36	0.11	0.19	0.79	0.97	0.92
	42055	23	0.23	0.05	0.07	0.36	0.13	0.27	0.84	0.98	0.86
	42001	23	−0.01	−0.18	−0.04	0.40	0.23	0.14	0.64	0.98	0.98
Norte 03	42003	23	0.00	−0.13	−0.11	0.21	0.20	0.18	0.82	0.93	0.94
	42055	23	0.09	−0.11	−0.13	0.49	0.19	0.19	0.64	0.98	0.98
	42001	46	0.25	0.09	0.11	0.38	0.22	0.21	0.73	0.88	0.91
Norte 04	42003	44	0.03	−0.13	−0.13	0.27	0.27	0.26	0.78	0.80	0.80
	42055	49	0.23	0.02	0.02	0.35	0.15	0.17	0.86	0.95	0.94

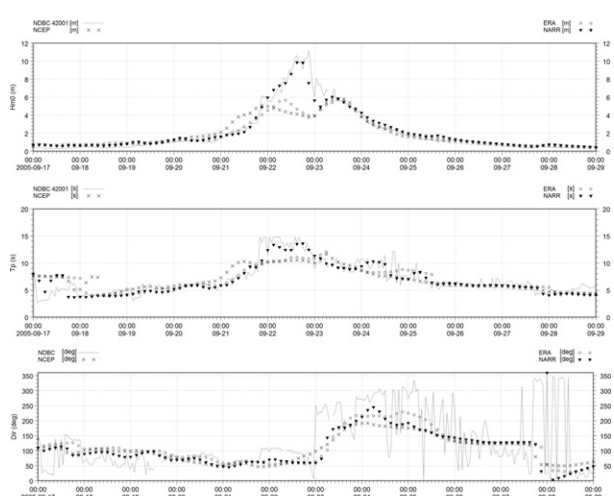

Fig. 7. Time series of observed and simulated SWH (upper panel), PWP (middle panel) and MWD (lower panel) during hurricane Rita.

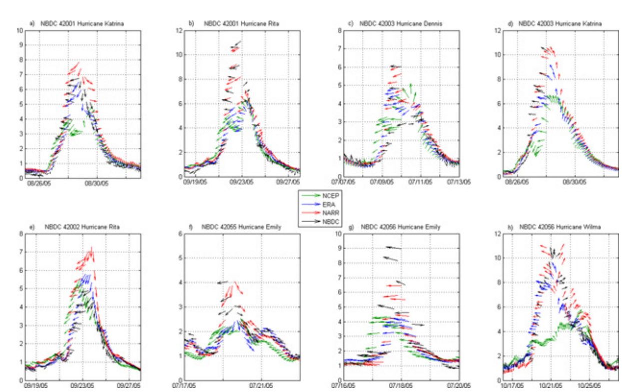

Fig. 8. Measured and simulated wave parameters during hurricane events at selected locations. PWP, SWH, and direction represented by vector length, origin and azimuth, respectively. (a) Katrina at 42001, (b) Rita at 42001, (c) Dennis at 42003, (d) Katrina at 42003, (e) Rita at 42002, (f) Emily at 42055, (g) Emily at 42056 and (h) Wilma at 42056.

3.3. Model-data comparisons: "Nortes" events

This section shows the wave model performance for the *Nortes* season from January through March. Contrary to cyclonic events, a general satisfactory performance for the three reanalyses is observed.

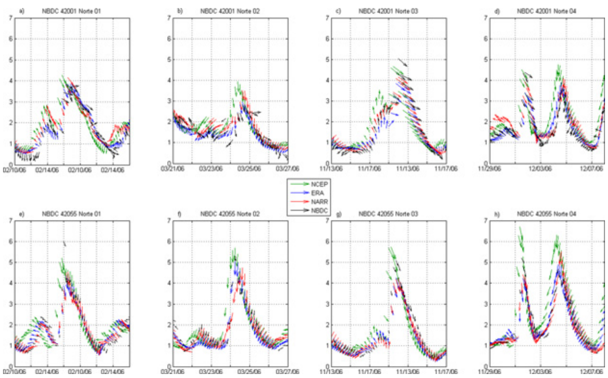

Fig. 9. Measured and simulated wave parameters during *Norte* events at selected locations. PWP, SWH, and direction represented by vector length, origin and azimuth, respectively. (a) *Norte* 01 at 42001, (b) *Norte* 02 at 42001, (c) *Norte* 03 at 42001, (d) *Norte* 04 at 42001, (e) *Norte* 01 at 42055, (f) *Norte* 02 at 42055, (g) *Norte* 03 at 42055 and (h) *Norte* 04 at 42055.

Table 6 shows the bias index, scatter index, and correlation coefficient, respectively, for the selected *Norte* events at different buoy locations. The bias index indicates that for most events there is an overestimation on SWH using the NCEP reanalysis, whereas ERA and NARR provide similar results. The scatter index shows a similar behavior, and the correlation coefficient shows excellent values for the NARR and ERA reanalyses and significantly lowers for the NCEP reanalysis.

As presented for the selected hurricane events, vector plots of SWH, PWP and MWD (Fig. 9) allow a visual inspection of the model performance for *Norte* events at the location of buoys 42001 and 42055. A good model estimate is obtained for the 3 wave parameters shown with the use of the 3 reanalyses, except for an overestimation of SWH using the NCEP reanalysis. Thus, NCEP, ERA, and NARR have in general a satisfactory performance when simulating waves generated by large scale meteorological systems such as *Nortes*.

3.4. Sensitivity analysis to reanalysis resolution

Despite an overall better statistical performance by ERA reanalysis over NARR, there is a continuous underestimation of SWH during hurricane events using ERA. Moreover, despite the wind speeds during hurricanes are very similar for NARR and ERA databases, the resulting hurricane generated SWH cannot be reproduced with ERA as accurately as with NARR (see Fig. 8). Since the NARR reanalysis has a higher spatial and temporal resolution (0.375° and 3 h) with respect to ERA (1.5° and 6 h) it was considered appropriate to test the wave model sensitivity to wind field resolution. An independent simulation using NARR with ERA spatial resolution (1.5°) has been conducted (the resolution was reduced by selecting one of every fourth grid point and the temporal resolution was kept 3 hourly). This allows investigating the effect of NARR wind fields with a 1.5° spatial resolution on the modeling of hurricane events. Fig. 10a–d shows a snapshot of the wind fields during hurricane Rita, as obtained from each of these two reanalyses, where it is clearly shown that the NARR provides a better qualitative representation of the cyclonic events. To contrast hurricane events with *Nortes*, Fig. 10e–h shows the wind fields during the *Norte 04* event, as obtained from the different reanalyses. The large scale structure of the *Norte* event is well represented from the three reanalyses, mainly because the wind speed and direction is homogeneous in such systems.

Fig. 11 shows the temporal QQ scatter plot for 2005 and 2006 simulation periods, suggesting that when the NARR wind fields are fed into the wave model with a coarse grid (similar to ERA – 1.5°) the higher SWH are underestimated, similar to the results using the ERA wind fields for the 2005 period. However, NARR results during 2006 are similar, irrespectively of the wind field resolution. This suggests that availability of ERA wind fields in a finer grid may improve wave simulations during cyclonic events, with the added advantage of having a global coverage.

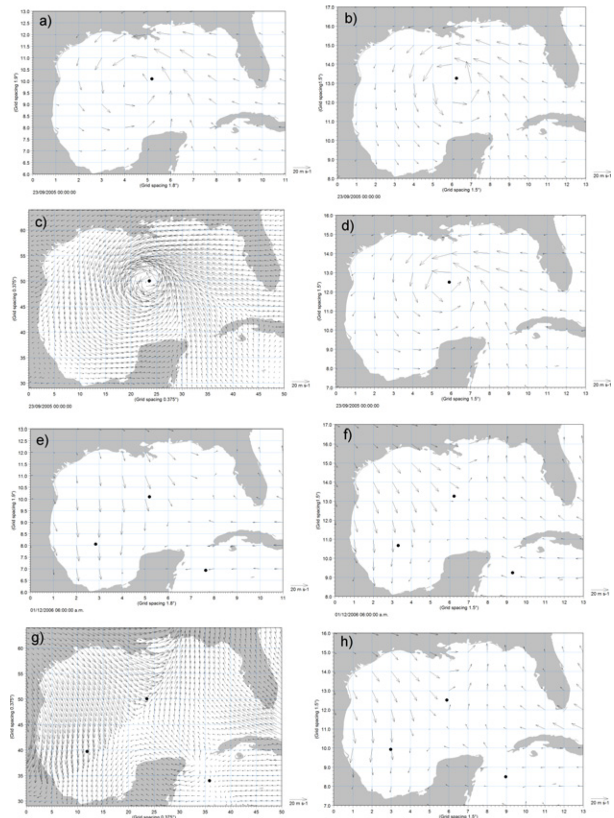

Fig. 10. Wind fields during hurricane Rita as defined by (a) NCEP, (b) ERA, (c) NARR, (d) NARR with ERA resolution and during *Norte* 04 as defined by (e) NCEP, (f) ERA, (g) NARR and (h) NARR with ERA resolution.

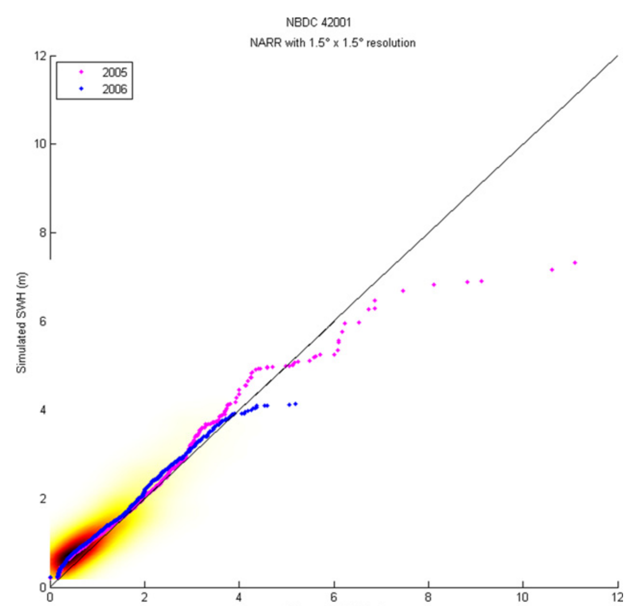

Fig. 11. Temporal (density contours) and QQ (dots) scatter plots of observed vs. simulated wind speed at NDBC 42001 during 2005 and 2006 using NARR data in ERA spatial resolution.

4. Conclusions

Long-term wave hindcasting accuracy in tropical regions is limited by the low spatial and temporal resolution of wind reanalysis for describing cyclonic events. Previous studies have proposed to compensate this underestimation by analyzing particular events and incorporating new techniques for determining winds fields during such events (e.g., blending hurricane wind fields). However, this may not be feasible for long-term wave hindcasting where detailed information on cyclonic events is not available. Thus, an assessment of the wind reanalyses was performed to investigate the current limitations of three different data sets. Numerical results suggest that the underestimation of wind speed by available reanalyses can be compensated in the wave model by reducing the energy loss due to whitecapping, i.e., reducing the C_{dis} coefficient. Although physically incorrect, the whitecapping parameters work as a fine tuning knob, providing better wave hindcast both for normal and extreme events. The calibration of the wave model was carried out in order to improve hindcast results for each of the wind reanalysis data set used. Therefore, the assessment of the wind reanalysis for wave modeling is not influenced by the model calibration. It was determined to use the same setup for the assessment of the wind reanalysis for wave modeling, considering such a setup was optimal for each database. It should be mentioned that while the C_{dis} coefficient is used as a calibration parameter, current efforts of the research group are being oriented toward the generation of more accurate wind fields under cyclone events and implementing a saturation limit to wave growth due to wind input.

Based on the statistical analysis, the assessment of three different wind reanalyses (NCEP, ERA and NARR) for its performance in wave modeling showed that the ERA and NARR reanalyses provided the best accuracy in terms of mean wave climate ($r^2 \sim 0.84$ for NCEP, $r^2 \sim 0.94$ for ERA interim, $r^2 \sim 0.92$ for NARR). However, the detailed analysis of extreme events shows that during cyclonic (hurricane) events the SWH is better reproduced using the NARR wind fields. Finally, all wind reanalysis (i.e., NCEP, ERA and NARR) resulted in a good representation of wave parameters when simulating extreme waves generated by large scale meteorological systems (e.g., *Nortes*). Despite differences in the atmospheric models used to determine the wind fields, it is shown that the spatial resolution has an important effect on the wave modeling by the fact that NARR improves the wave modeling under hurricane events as compared with lower spatial resolution simulations.

Acknowledgements

The present study was supported by CONACYT-FOMIX-YUC project-106400 and project 1361 from the Instituto de Ingeniería – UNAM. NCEP and NARR Reanalyses data provided by the NOAA/OAR/ESRL PSD, Boulder, Colorado, USA, at http://www.esrl.noaa.gov/psd/; and ERA-interim Reanalysis data provided by the ECMWF at http://data-portal.ecmwf.int/data/d/interim_full_daily. The authors would also like to thank DHI Water & Environment for facilitating a University License of MIKE 21 SW and the two anonymous reviewers who greatly contributed to the improvement of this manuscript.

References

[1] Sørensen O.R., Kofoed-Hansen H., Rugbjerg M., Sørensen L.S. A third-generation spectral wave model using an unstructured finite volume technique. In: J.M. Smith (Ed.) Proceedings of the 29th international conference on coastal engineering. ASCE Lisbon, Portugal; 2004, pp. 894–906.

[2] Booij N., Ris R.C., Holthuijsen L.H. A third-generation wave model for coastal regions. 1. Model description and validation. Journal of Geophysical Research. 1999;104:7649–7666.

[3] Tolman HL. User manual and system documentation of WAVEWATCH III version 3.14. Technical Note 276. NOAA/NWS/NCEP/MMAB; 2009. p. 194.

[4] Komen G.J., Cavaleri L., Doneland M., Hasselmann K., Hasselmann S., Janssen P.A.E.M. Dynamics and modelling of ocean waves. Cambridge University Press UK; 1994.

[5] Cardone V.J., Graber H.C., Jensen R.E., Hasselmann S., Caruso M.J. In search of the true surface wind field in SWADE IOP-1: ocean wave modelling perspective. The Global Atmosphere and Ocean System. 1995;3:107–150.

[6] Dee D.P., Uppala S.M., Simmons A.J., Berrisford P., Poli P., Kobayashi S. The ERA-interim reanalysis: configuration and performance of the data assimilation system. Quarterly Journal of the Royal Meteorological Society. 2011;137:553–597.

[7] Swail V.R., Cox A.T. On the Use of NCEP-NCAR Reanalysis Surface Marine Wind Fields for a Long-term North Atlantic Wave Hindcast. Journal of Atmospheric and Oceanic Technology. 2000;17:532–545.

[8] Cox A.T., Swail V.R. A global wave hindcast over the period 1958–1997: validation and climate assessment. Journal of Geophysical Research. 2001;106:2313–2329.

[9] Weisse R., Günther H. Wave climate and long-term changes for the Southern North Sea obtained from a high-resolution hindcast 1958–2002. Ocean Dynamics. 2007;57:161–172.

[10] Wang X.L., Swail V.R. Trends of Atlantic wave extremes as simulated in a 40-yr wave hindcast using kinematically reanalyzed wind fields. Journal of Climate. 2002;15:1020–1035.

[11] Pilar P., Soares C.G., Carretero J.C. 44-Year wave hindcast for the North East Atlantic European coast. Coastal Engineering. 2008;55:861–871.

[12] Wang X.L., Swail V.R., Zwiers F.W. Climatology and changes of extratropical cyclone activity: comparison of ERA-40 with NCEP–NCAR reanalysis for 1958–2001. Journal of Climate. 2006;19:3145–3166.

[13] Caires S., Sterl A., Bidlot J.-R., Graham N., Swail V. Intercomparison of different wind-wave reanalyses. Journal of Climate. 2004;17:1893–1913.

[14] Spindler DM, Tolman H. Example of WAVEWATCH III for the Alaska area. Technical note. Environmental Modeling Center; 2010. p. 17.

[15] Siadatmousavi S.M., Jose F., Stone G.W. The effects of bed friction on wave simulation: implementation of an unstructured third-generation wave model, SWAN. Journal of Coastal Research. 2011:140–152.

[16] Siadatmousavi S.M, Jose F., Stone G.W. Evaluation of two WAM white capping parameterizations using parallel unstructured SWAN with application to the Northern Gulf of Mexico, USA. Applied Ocean Research. 2011;33:23–30.

[17] Saha S., Moorthi S., Pan H.-L., Wu X., Wang J., Nadiga S. The NCEP climate forecast system reanalysis. Bulletin of the American Meteorological Society. 2010;91:1015–1057.

[18] Weisse R., Feser F. Evaluation of a method to reduce uncertainty in wind hindcasts performed with regional atmosphere models. Coastal Engineering. 2003;48:211–225.

[19] Cavaleri L., Alves J.H.G.M., Ardhuin F., Babanin A., Banner M., Belibassakis K. Wave modelling – the state of the art. Progress In Oceanography. 2007;75:603–674.

[20] Hasselmann K. On the spectral dissipation of ocean waves due to white capping. Boundary-Layer Meteorology. 1974;6:107–127.

[21] Komen G.J., Hasselmann K. On the existence of a fully developed wind-sea spectrum. Journal of Physical Oceanography. 1984;14:1271–1285.

[22] Janssen P.A.E.M. Wave-induced stress and the drag of air flow over sea waves. Journal of Physical Oceanography. 1989;19:745–754.

[23] Ardhuin F., Rogers E., Babanin A.V., Filipot J.-F., Magne R., Roland A. Semiempirical dissipation source functions for ocean waves. Part I. Definition, calibration, and validation. Journal of Physical Oceanography. 2010;40:1917–1941.

[24] SWAN-team. SWAN Cycle III version 40.85. Scientific and technical documentation; 2011.

[25] van der Westhuysen A.J., Zijlema M., Battjes J.A. Nonlinear saturation-based whitecapping dissipation in SWAN for deep and shallow water. Coastal Engineering. 2007;54:151–170.

[26] Moon I.-J., Ginis I., Hara T. Impact of the reduced drag coefficient on ocean wave modeling under hurricane conditions. Monthly Weather Review. 2008;136:1217–1223.

[27] Amante C, Eakins BW. ETOPO1 1 arc-minute global relief model: procedures, data sources and analysis. NOAA Technical Memorandum NESDIS NGDC-24; 2009. p. 19.

[28] DHI. MIKE 21. Spectral wave module. Scientific documentation. DHI Water & Environment; 2011.

[29] Kalnay E., Kanamitsu M., Kistler R., Collins W., Deaven D., Gandin L. The NCEP/NCAR 40-year reanalysis project. Bulletin of the American Meteorological Society. 1996;77:437–471.

[30] Simmons A, Uppala S, Dee D, Kobayashi S. ERA-interim: new ECMWF reanalysis products from 1989 onwards. ECMWF Newsletter; 2007:25-35.

[31] Mesinger F., DiMego G., Kalnay E., Mitchell K., Shafran P.C., Ebisuzaki W. North American regional reanalysis. Bulletin of the American Meteorological Society. 2006;87:343–360.

[32] Schultz D.M., Bracken W.E., Bosart L.F., Hakim G.J., Bedrick M.A., Dickinson M.J., et al. The 1993 superstorm cold surge: frontal structure, gap flow, and tropical impact (1996). Monthly Weather Review 1997;125:5-39 .[Corrigenda, 125, 662]

[33] Reding PJ. The Central American cold surge: an observational analysis of the deep south-ward penetration of North American cold fronts. MSc thesis, Texas A&M University; 1992.

[34] Rosengaus M., Jiménez M., Vázquez M.T. Atlas climatológico de ciclones tropicales en México. Centro Nacional de Prevención de Desastres, Instituto Mexicano de Tecnología del Agua; 2002. p.106.

[35] Beven J.L., Avila L.A., Blake E.S., Brown D.P., Franklin J.L., Knabb R.D. Atlantic hurricane season of 2005. Monthly Weather Review. 2008;136:1109–1173.

[36] Trenberth K.E., Shea D.J. Atlantic hurricanes and natural variability in 2005. Geophysical Research Letters. 2006;33.
[37] López-Méndez J.V. Análisis del evento meteorológico del 2007 relacionado con la inundación de Tabasco. Universidad Nacional Autónoma de México; 2009.
[38] Franklin J.L., Brown D.P. Atlantic hurricane season of 2006. Monthly Weather Review. 2008;136:1174–1200.
[39] NDBC. Handbook of Automated Data Quality Control Checks and Procedures. NDBC Technical Document 09– 02. National Oceanic and Atmospheric Administration – National Data Buoy Center; 2009.
[40] Moeini M.H., Etemad-Shahidi A. Application of two numerical models for wave hindcasting in Lake Erie. Applied Ocean Research. 2007;29:137–145.
[41] Chao Y.Y., Alves J.-H.G.M., Tolman H.L. An operational system for predicting hurricane-generated wind waves in the North Atlantic Ocean. Weather and Forecasting. 2005;20:652–671.
[42] Jose F., Kobashi D., Stone G.W. Spectral wave transformation over an elongated sand shoal off South-Central Louisiana, U.S.A. Journal of Coastal Research. 2007:757–761.